Determination of Impact Stress on the Superior Surface of Ex-vivo Porcine Vocal Folds using Digital Image Correlation

By

Jonathan Young, MDCM, FRCSC

Department of Otolaryngology – Head and Neck Surgery

McGill University, Montreal, Canada

December, 2012

A thesis submitted to McGill University in partial fulfillment of the requirements of the degree of Master of Science

Acknowledgements

I would like to thank Dr. Luc Mongeau for his basic science supervision and support for all aspects of this project. I would like to thank Dr. Sam Daniel and Dr. Mindy Black for their clinical supervision, and their continued mentorship and support for this project. I would like to thank Gil Rind and Jennifer Robb. These undergraduate students designed much of the experimental apparatus, and provided immeasurable guidance by performing the experiments together with me. I would like to thank Olymel, the pork factory which provided the larynges; This study was supported by the Canadian Institute for Health Research.

TABLE OF CONTENTS

PAGE

LIST OF FIGURES

Page

LIST OF TABLES

Nomenclature

DIC: Digital Imagery Correlation

EGG: Electroglottography

LCA: Lateral cricoarytenoid muscle

PCA: Posterior cricoarytenoid muscle

PGG: Photoglottography

TVF: True Vocal Fold

LP: Lamina Propria

ABSTRACT

Mechanical stresses in the vocal folds during phonation are caused in part by impact forces associated with collision between the vibratory surfaces. These stresses may be responsible for the formation of nodules, polyps and cysts. The objective of this study was to investigate a method for measuring impact stress non-invasively.

High-speed images of porcine larynges were studied using Digital Image Correlation (DIC), a method used to measure strain fields by tracking random speckle pattern deformations. Impact stresses may be estimated from the resulting data through the use of a Hertzian impact model and the elastic properties of the tissue. Methods to improve the speckling pattern for excised tissue were developed. Two dyes were found to produce speckles with a desirable Gaussian greyscale distribution, and good adhesion to the tissue.

Superior surface strain results were obtained for two porcine larynges. The strain values obtained in a few regions of the superior surface were found to be comparable with previous results from a mechanical silicone model. Further work with animal models is needed in order or perfect the speckling procedure and to obtain more uniform results over the superior surface.

Although challenges still exist before a similar method can be used with human subjects, these preliminary results suggest that DIC displays some potential for future clinical use.

Chapter 1: Background

This chapter provides background to the material presented in this thesis. Phonotrauma and benign laryngeal lesions are described. A review of the literature on contact pressure studies is presented. The objectives of the project are defined.

1.1 Clinical Background

1.1.1 Benign Laryngeal Lesions

Phonotrauma, defined as vocal abuse, misuse, and overuse is postulated to be the etiology behind vocal fold nodules (fig. 1.1a), cysts (fig. 1.1b) and polyps (fig. 1.1c)[1-3]. These benign, common lesions may cause voice hoarseness, throat discomfort and pitch breaks. They are frequent and significant in professional voice[4] (fig. 1.1).

1.1.2 Anatomical Nomenclature

The true vocal fold (TVF) is a layered structure, as illustrated in fig. 1.2. The vocal cover includes the epithelium and superficial lamina propria(SLP). The cover envelopes the vocal ligament, which consists of the intermediate (ILP) and deep layers (DLP) of the lamina propria. The superficial lamina propria consists of an amorphous gelatinous-like material, which undergoes shear deformations due to transverse motion of the mucosal cover and the vocal ligament. The vocalis muscle[5] is the deepest layer of the structure, and is responsible for vocal fold adduction. Remodeling of the lamina propria and to a lesser degree, the epithelium, is the pathology behind the formation of phonotraumatic lesions[6].

1.1.3 Physiology of Voice Production

During normal breathing, the vocal folds are abducted (open position), allowing air to move from the oral and nasal cavity to the lungs (fig. 1.3). During phonation, the vocal folds are adducted, i.e. they meet in the midline as shown in fig. 1.4. Air flows through the glottis when the subglottal air pressure reaches a certain critical value, called the onset pressure. During voice production, air flows from the subglottic to the supraglottic region. The vibratory motion of the vocal folds features the propagation of a mucosal wave (fig. 1.5). The mucosal wave is a structural surface wave that propagates in the inferior-superior direction. The mucosal wave is designed to control airflow through the glottis. When air is transmitted, sound is produced, as the subglottic air collides with a still column of air above the glottis. The mucosal wave propagates at a frequency of approximately 120 Hz in the average male, and approximately 220 Hz for an average female. It is believed that benign lesions of the vocal folds are caused by contact stresses and trauma during normal or pressed phonation[7-9]. Such trauma leads to alterations in the biochemical pathways responsible for epithelial and basement membrane maintenance[10-13]. This ultimately leads to the formation of phonotraumatic lesions, namely nodules, polyps, and cysts. In addition, stiffening/scarring of the medial vocal fold edge causes a loss of compliance of the superficial lamina propria. This affects voice quality and clarity by altering and disordering the mucosal wave propagation.

1.1.4 Treatment of Benign Vocal Fold Lesions

The treatment of nodules, polyps and cysts may be non-surgical. Speech and/or singing therapy may reduce vibratory trauma by diminishing muscle tension and abusive vocal behaviors such as loud voicing and throat clearing [14-5]. The reduction of agravating factors, such as smoking

cessation or treatment of laryngopharyngeal reflux, should be initiated as well. If these treatments fail, surgical intervention is warranted. This involves the excision of the lesion[16], typically followed by a period of voice rest. This could also include a trial of voice therapy. Different methods for surgical excision are available. Surgical methods include cold steal excision, laser therapy, and corticosteroid injection.

1.1.5 Impact Stress

Stresses are a measure of internal mechanical forces on a deformable body. Many components of stresses play a role during vocal fold vibrations. These include shear stress in the tissue, aerodynamic stresses in the fluid, tensile stresses, contractile stresses, and inertial stresses[17]. Shear stress is a force that acts in a direction parallel or tangential to the surface of the material. Tensile stress is the stress state leading to expansion or increase in volume of a material. Impact stresses are generated in the vocal fold tissue during collision of the vibratory surfaces These are believed to be the strongest contributor to voice trauma[11].

1.1.6 Imaging Techniques

Tools that provide clear and precise views of the larynx include rigid endoscopy and flexible endoscopy with chip-tip technology. These tools yield detailed digital images that may be used to estimate the fundamental frequency of oscillations[18]. Computer software may be used to analyze jitter (perturbations in the frequency) and shimmer (perturbations in the amplitude). Little information is provided by standard physical exams about impact stress. Recent work has been done to estimate impact stresses from high speed digital video endoscopy[19]. Direct measurements are challenging. Phonation, airway protection and respiration comprise the three

main functions of the human larynx. Protection of the airway and lungs from aspirating foreign materials which can lead to airway obstruction and/or pneumonia is of vital importance. Thus, the insertion of any foreign object or material in between or near the vocal folds often causes a cough reflex or laryngospasm, unless the true vocal folds are properly anesthetized.

Although it seems clear that impact stress is instrumental in the formation of nodules, polyps and cysts, the absence of a reliable and accurate method to measure impact stresses hampers the development of quantitative metrics. Could a certain amount of voice use or a particular volume intensity level produce an impact pressure great enough to produce a phonotraumatic lesion or vocal fold hemorrhage? This could be defined as a dose of voicing at which these lesions will be produced[20]. A technology for impact pressure measurements would be beneficial to the otolaryngologist and the speech therapist. A knowledge of the impact stresses in patients and comparisons to normative data, may lead to strategies to reduce stress within the larynx, thus diminishing the incidence of, and helping in, the non-surgical therapy of nodules, polyps or cysts. This technology may help the identification of early lesions that are difficult to identify clinically. Such technology may be used for fundamental research on the vibratory cycle. The effects of these lesions on phonation could be studied and better understood, leading to improved treatments.

Previous work has been done to study the impact stresses within the vocal folds during phonation. Finite element models have been used to estimate impact stresses[21]. Cadaveric animal hemi-larynges have been used with pressure transducers embedded in the side wall to measure impact pressure[22]. Similar anatomical properties between human and canine larynges have led to the use of canine models as a research tool. Numerous research groups have investigated methods to measure impact stress in live human subjects[23-5]. Most of these attempts are clinically

challenging, because they are applicable only to hemi-larynges, or they are difficult to tolerate for the patient.

1.2 Literature Survey

Previous impact stress studies are reviewed and organized according to the laryngeal model utilized for experimentation. These include finite element models, physical models, excised cadaveric larynges (human, animal), and *in vivo* studies of live human subjects.

1.2.1 Cadaveric Larynges

Research groups have previously used animal models to measure impact stresses during phonation. Jiang and Titze[22] measured impact stresses using excised canine larynges. Their experimental set-up involved a hemi-larynx, with the right vocal fold oscillating against a plexiglass plate with imbedded pressure transducers. The glottal waveform was divided into three separate phases, namely the impact phase, the pre-open phase and the open phase. The impact phase is the portion of the cycle when the vocal fold first contacts the plexiglass surface. Peak pressures were found to be in the order of .5 - 5 kPa, at the midmembranous portion of the vocal fold. The vocal folds were then lengthened to simulate a falsetto voice. The impact stresses at the midline were then negligible, because the folds did not contact each other at the midline. It was thus assumed that falsetto voices would lead to a reduced incidence of nodules. This is supported by recent clinical evidence that specific vocal fold postures may enhance the degree and speed of healing, and limit the amount of local inflammation[27]. The need for sensors on the

vocal fold surface constitutes the major limitation of this approach. The stress and strain are measured at specific points along the medial surface of the folds only. Measurements over the entire surface of the folds are needed.

Non-invasive animal cadaveric impact stress measurements have included photoglottography (PGG) and electroglottography (EGG). PGG is a measure of the relative displacement of the vocal folds. By calculating the first and second derivatives of the PGG displacement waveforms, the velocity and acceleration of the vocal folds were estimated for cadaveric animal larynges[26]. Impact forces may be estimated from the acceleration through the impulse momentum theorem[36]. The experimental set-up included a pressure transducer that was placed between the vocal folds during phonation. The directly measured impact stress was compared to the second derivative of the PGG signal. In all nine canine larynges studied, there was a linear and positive relationship between the acceleration and the impact stress. Although the relationship was positive and linear for each of the nine larynges, the governing equation was different in each case. Verdolini et al.[28] attempted to correlate the EGG close quotient (EGG CQ) with the contact pressure. The EGG CQ is defined as the ratio of the time period for which the glottis is closed and the oscillation period. The results suggested the usefulness of EGG CQ as a first cut measure of the contact pressure for individual subjects.

Alipour and Jaiswal[29] studied the mechanical properties and phonatory characteristics of porcine, sheep and canine larynges. The air flow supplied was humidified at 100% and at body temperature (37^0 Celsius). The larynges were mounted in a supporting frame. Sutures were placed in the lateral cricoarytenoid muscle to allow the adduction of the vocal folds using a weight-pulley assembly system. Porcine models produced higher frequencies than other animals. Comparative anatomy has displayed certain key similarities to human larynges[16]. The porcine

larynx is divided in two layers of lamina propria, while the human larynx features a three-layer system. The porcine vocal fold has a stiffness similar to that of the human vocal folds. The collagen and elastin in the porcine lamina propria is similar to that of humans. In addition, the porcine mucosal thickness, which is .9 mm, is similar to the human thickness of 1.1 mm. The intrinsic muscles of the porcine larynx have origins and insertions similar to those of the human larynx.

1.2.2 Synthetic Models

Physical replicas of the human vocal folds have been used to investigate the mechanics of voice production. These are typically made of silicone rubber[30]. Digital image correlation was used to determine the strain field and the strain rate on the superior surface of a self-oscillating physical model of the vocal folds using a Hertzian impact model[31]. The stress fields on the superior surface and the contact pressures were determined from the strain field, based on the assumption of incompressible material. The peak contact pressure for the physical model was found to be 0.7 kPa for a subglottal pressure of 1.2 kPa. The stress measured on the superior surface of the vocal folds during collision was tensile. Impact stress may also be estimated by analysis using a finite element model[32]. Such models suggest that there may be an over-estimation of contact pressures due to the lack of consideration of the saturation of strain values at higher flow rates.

1.2.3 Finite Element Models

Vocal fold tissue is deformable, it changes shape when a force is applied on it. The finite element model method has been used to model or predict the deformation of vocal fold tissue under mechanical load. The deformable vocal fold is modeled as a collection of lumped rigid

mass elements linked by springs. The stiffness of the springs may be adjusted to obtain the required material properties. The main disadvantage of the finite element model is the computational cost[32]. Chen et al.[32] reported a nine day period for computational analysis. In addition, computational errors occurred when the model medial surface was subjected to both pressure loads and contact.

Gunter et al.[21] used a finite element model to predict the collision force between one vocal fold and the rigid surface of a hemilarynx physical model. The vocal fold material was assumed to be linear elastic, since the deformations observed were small. The material was also assumed to be isotropic, with elastic moduli obtained from previous studies. The glottal closure dynamics and collision forces obtained from the model were comparable to experimental results. For subglottal pressures of 1.5 kPa and 2.0 kPa, the contact forces predicted were 20 and 30 kPa respectively, and the contact areas were 35 mm^2 and 27 mm^2 respectively. The values measured in these experiments were similar to previous data recorded by Jiang and Titze[22].

1.2.4 In Vivo Measurements

Verdolini et al.[23] performed direct contact pressure measurements in twenty live subjects. Impact stress was measured for different voice qualities, pitches and intensities using a pressure sensor introduced between the vocal folds at the midmembranous portion. Synchronous electroglottographic (EGG) was used to estimate the closing quotient, and assess the potential for this technique to measure impact stress. Anesthesia was provided with direct swabbing of the vocal folds. A total of seventeen patients completed the study. Two were eliminated secondary to strong gag reflexes. A third patient was eliminated due to secretions. Ten patients did not meet acceptable criteria for use in the study due to difficulties with reliable placement of pressure

sensors as assessed by endoscopic examination. Thus, only seven of the twenty patients enrolled in this study yielded analyzable data. There were no major complications, although one patient suffered multiple 1 mm hemorrhagic spots on the vocal folds and a cough reflex. These had subsided completely at a two week follow-up appointment. The measured impact stress values ranged from less than 1 kPa to approximately 3 kPa. The sensor was 0.4 mm thick, and may have altered vocal fold vibrations. Only 35% of the subjects data was considered accurate and reportable. No clear correlation could not be obtained between glottographic closed quotient and contact pressure .

Gunter et al.[24] performed measurements using a sensor with a thickness of .29 mm. They obtained data for three out of five patients. One patient did not tolerate sensor placement. One subject's glottic view was obstructed by supraglottic tissue from previous airway reconstructive surgery. Two out of the three patients for which reportable data was obtained had unilateral vocal fold immobility, thus facilitating sensor placement and subsequent measurements. The peak pressures correlated mostly with the intensity of the voice, as shown in fig. 1.6. Challenges reported in this study included the difficulty to obtain measurable data in the mid-membranous region due to sensor length, and to stabilize the sensor. Sensor modifications were proposed.

In a recent study, Chen et al.[32] performed direct measurements of contact pressures using a probe microphone. Different voice types, including breathy (abducted), normal (equal abduction and adduction) and pressed voices (hard adduction) were studied. At 70 db sound pressure level (SPL), normal and breathy voices exhibited similar contact pressures of .25 and .26 kPa respectively. Contact pressures for the pressed voice were stronger, and measured to be .7 kPa. As for transoral probes, there were issues with patient tolerance and probe placement. In

addition, the probe was found to interfere with vocal fold oscillation, which may have caused an under-estimation of the amplitudes when compared to previous studies.

The use of pressure sensors placed between the vocal folds is difficult to implement for a clinician for several reasons. The time of procedure is lengthy. The process of anesthetizing and examining/measuring impact stress is lengthy. In addition, the cost/benefit ratio may be prohibitively high since only approximately one in two patients tolerates the procedure that yields reproducible and reliable data. Investigations of other non-invasive methods are thus warranted.

1.2.5 Medical Applications of DIC

The digital image correlation (DIC) method has been used to measure strain and displacement in biological tissues other than the larynx. Zhang[33] used DIC to measure the deformation of the arterial tissue from a bovine aorta in uniaxial tension. DIC analysis has been used in obtaining measurements of stress and strain fields in bone tissue, although digital speckle pattern interferometry is capable of measuring smaller strain. Later, Sutton[34] used DIC to measure the strain field on mouse carotid arteries. Since the diameter of the arteries in the experiment was very small (0.40mm diameter) the 3D DIC system was coupled to a microscope to effectively measure the small deformation.

1.2.6 Research Objectives & Study Rationale

The objective of the current research study is to help clarify a clinical method of measuring impact stresses on the vocal folds that is easily performed, reproducible, and accurate. As

previously stated, there is a definite clinical indication for a non-invasive method to measure impact stresses in vocal folds. The rationale for the development of DIC as a means of measuring impact stress is that is that it is a non-invasive examination, and theoretically should be well tolerated by the patient. In addition, the analysis can be performed rapidly, providing useful clinical data in moments. The present study utilizes digital image correlation to analyze surface tensions and strains on cadaveric porcine larynges.

a)

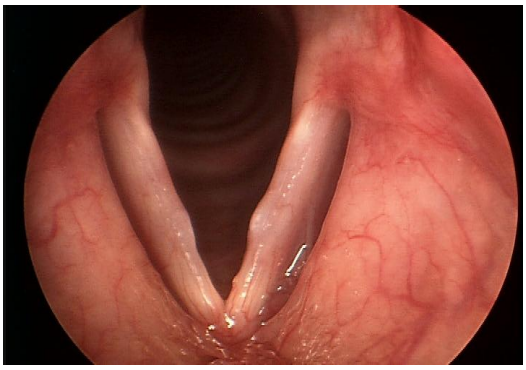

b)

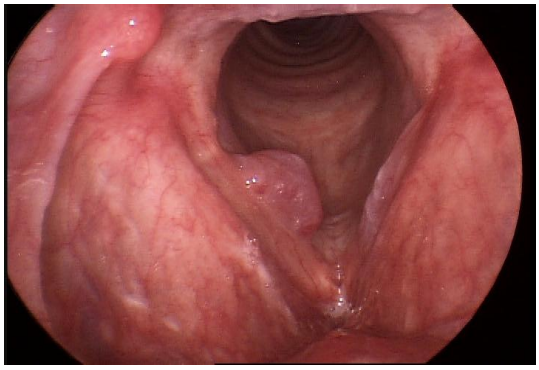

c)

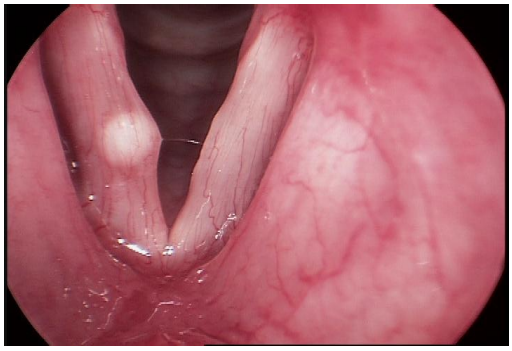

Figure 1.1 Vocal fold nodules (a), polyps(b), and cyts (c).

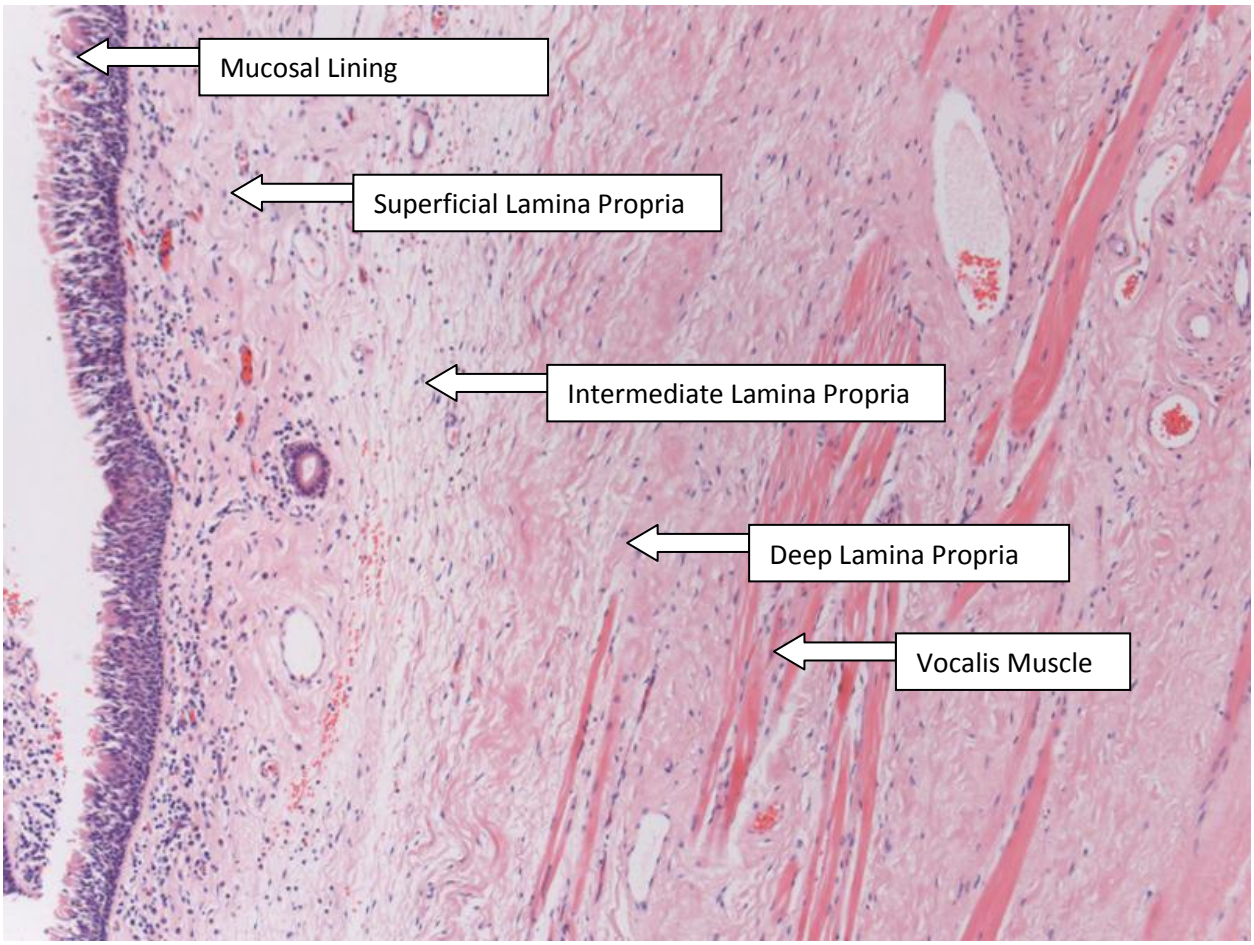

Figure 1.2 Hematoxylin and Eosin histological section of the layered microstructure of the true vocal folds.

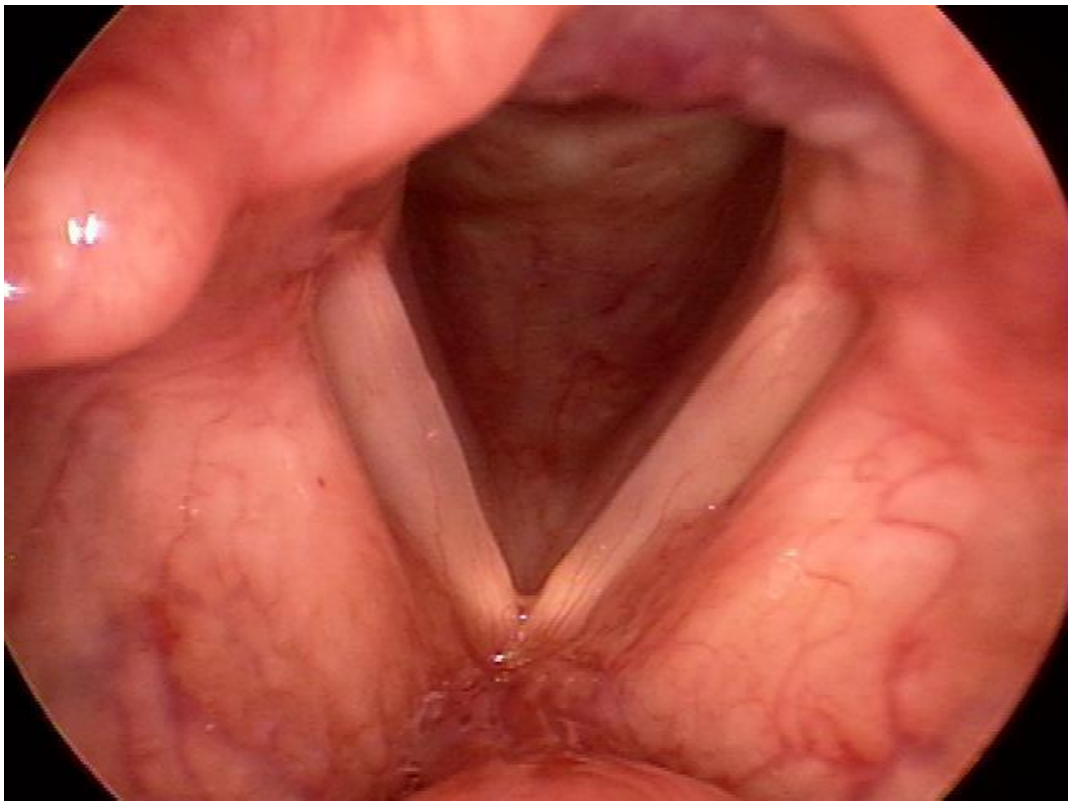

Figure 1.3 The vocal folds during normal respiration in the abducted position.

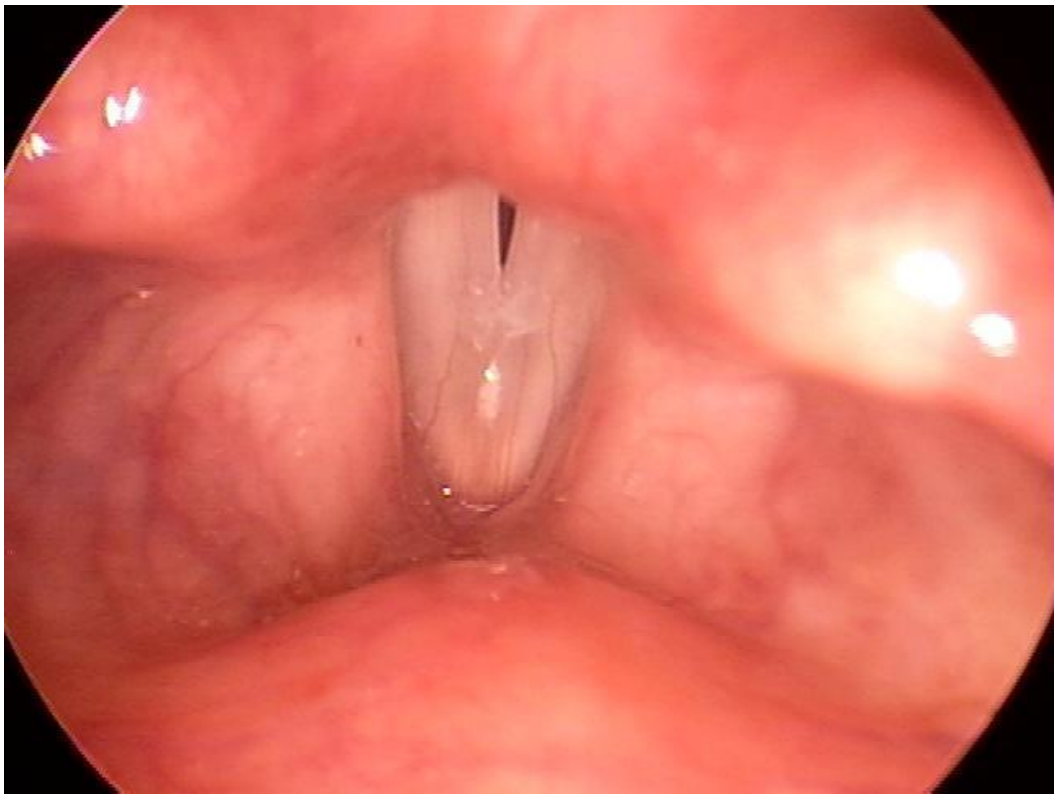

Figure 1.4 The vocal folds contacting each other during phonation in the adducted position.

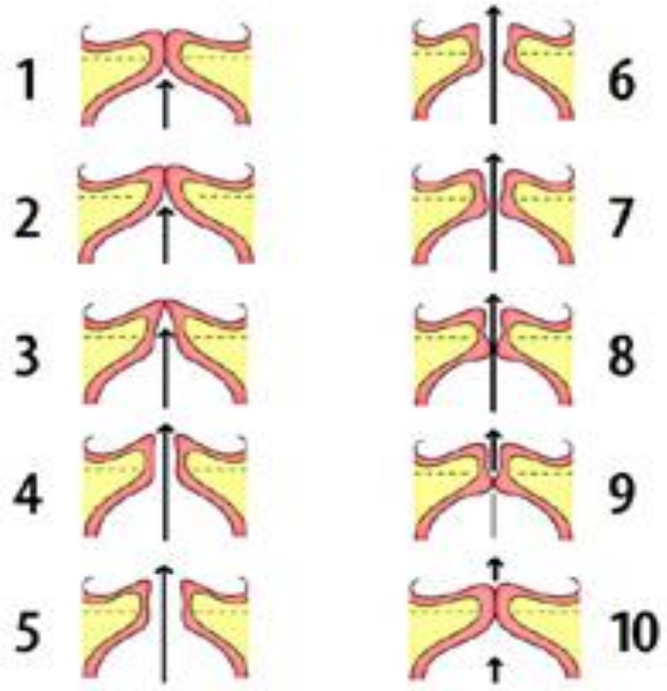

Figure 1.5 Schematic of the mucosal wave. The point of contact is on the medial surface of the true vocal folds. This is the location of contact lesions, which include polyps, nodules and cysts.

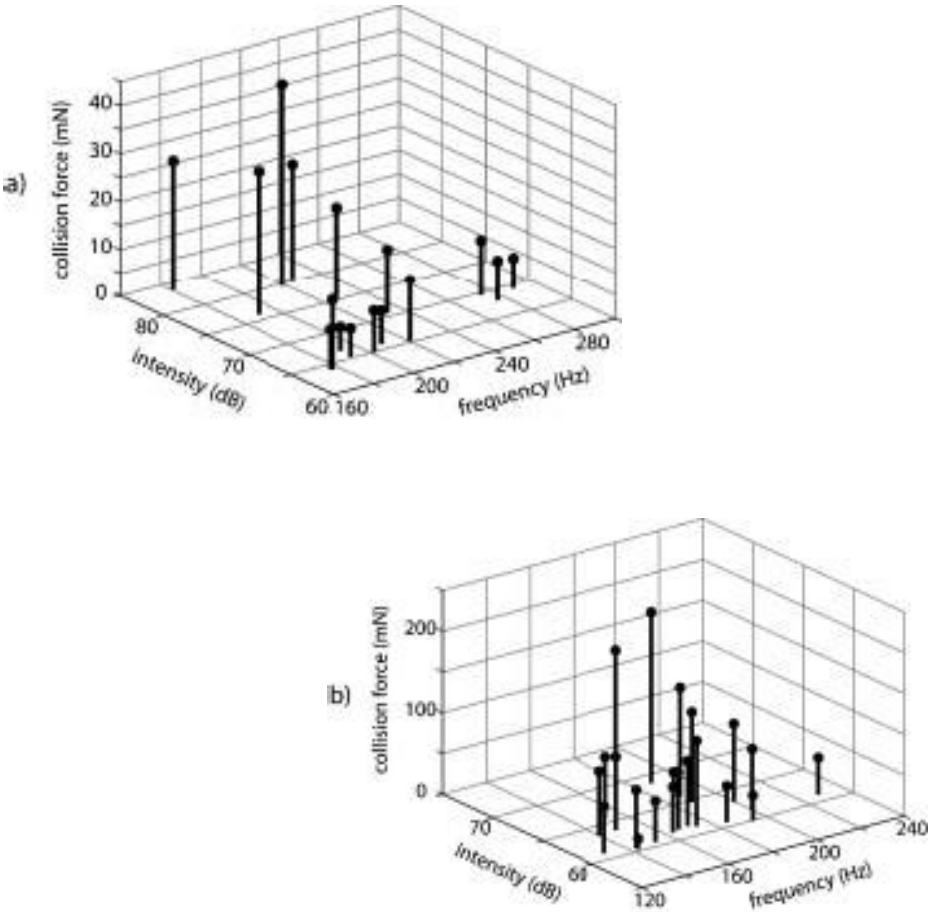

Figure 1.6 Scatter plots of 2 male participants displaying intensity versus frequency versus collision forces. Increasing impact stresses are noted with increasing intensity. There is no correlation between frequency and impact stress (Used with permission from Gunter et al, 2005).

Chapter 2: Experimental Methods

2.1 The experimental Model

2.1.1 Ethics

Use of cadaveric porcine larynges was approved by the McGill animal care committee.

2.1.2 The Porcine Model

Porcine larynges were obtained from Olymel, a pork production factory. Pigs had been sacrificed within 24 hours of retrieval. The larynges were removed from the rest of the trachea, which was sent for incineration. The larynges were transported from Olymel to the biomedical engineering laboratory at McGill University in a plastic container containing normal saline solution. Preparation of the porcine larynx was performed by first removing the surrounding soft tissues, including the strap muscles, in addition to the thyroid gland which was often a part of the specimen (Fig. 2.1 A, B). Following this, the supraglottic structures were removed to reveal the true vocal folds (Fig. 2.1 C). This was performed by incising the thyroid cartilage in the midline to the level of the false cords, then extending the incision laterally to remove most of the superior portion of the larynx. The false cords were then gently dissected and removed to reveal the TVFs. The posterior glottis, which contains a large gap that leads to an accessory cartilage not contained in human larynges, was sutured in a running fashion using 3-0 vicryl sutures (Fig. 2.1 C). One single suture was placed on the posterior portion of the vocal folds to emulate vocal fold adduction. Careful dissection of paralaryngeal tissues, including the strap muscles, left exposed cartilage on the exterior surface of the larynx. This proved to be effective in stabilizing the larynx to the external frame, as any muscle left on the surface of the larynx would lead to

movements of the larynx during airflow. The trachea was excised up to approximately the third tracheal ring. Gauze on a large hemostat was used to dry the subglottis and trachea, in order to prevent dilution of the dye. Dry air was blown through the larynx to dry the subglottis, and to search for leaks which could be stitched. All larynges were utilized on the day of harvest in order to minimize deterioration of the specimen. The specimens were then placed in a freezer after use. The McGill department of biohazards handled all used larynges and disposed of them.

2.2. Method of analysis

2.2.1 Digital Image Correlation

Images were obtained and analyzed using Digital Image Correlation hardware and software. Strain was obtained from the analysis of grayscale patterns from a reference image location to successive deformed images (fig. 2.2 A, B). The reference image was typically the item or area of interest at rest, prior to oscillations. A randomized speckle pattern was applied on the deformable solid on the area to uniquely identify each material point. As multiple pixels may have the same grayscale value, the program analyzed a square of pixels of predetermined size and calculated the strain as the square was deformed.

The software used for this experiment was a commercially available tool, Vic-2D by Correlated Solutions. This software calculates the strains and displacements on the visible surface. Images were obtained during oscillation, and compared with a reference image of the larynx at rest. Speckling of the dye is optimal when the gray-scale distribution of the surface of the image of interest is distributed along a normal Gaussian bell curve. A randomized speckle pattern is important to satisfy this requirement. If the pattern is too monotonous or too vague, it is difficult

to obtain proper results from DIC analysis. The software then divides the image in to smaller areas of analysis termed subsets. The subset size for the analysis was varied between 19x19 and 25x25 pixels. A step of one pixel and a quintic spline interpolation were used in the analysis. If the area selected is too small, it is difficult to find a unique pattern that is not repeated in the picture. If the area selected is too large, the results are spatially averaged. The step size is the number of pixels in the stencil used in the pixel interpolating a scheme. A subset size of one yields the highest resolution and therefore the most accurate results. A quintic spline was selected because it is the highest order approximation available, which yields the closest approximation to the grayscale patterns in the picture. The displacements and strains were then overlayed onto the reference image, permitting estimation of the strain at various locations over one oscillation cycle.

2.3 Speckle Creation

2.3.1 Dye Slection

A dye was needed to generate a speckle pattern with a Gaussian grey scale distribution. The ideal dye for the purpose of this study would adhere onto the surface of the vocal fold, without diffusing into the tissues. Dye diffusion results in a uniform distribution that is not appropriate for analysis by the digital image software (VIC 2D). The properties of the dye must therefore be slightly hydrophobic, as the vocal folds are strongly hydrophilic. The ideal dye must also be non-toxic in order to be applicable to in-vivo usage.

A literature search was performed to find dyes that were commonly used in medical applications. Dyes with known minimal toxicity were also tested. In addition to dyes, cosmetics such as

foundation sprays (ERA face) and powders, as well as food dyes were tested. Powdered dyes such as methylene blue and congo red were tested with multiple solvents (water, corn syrup, barium) (see table 2.1).

Analysis of the speckle quality was performed on excised porcine larynges, as previously described. Grey scale analysis was performed using adobe photoshop CS2, as shown in fig. 2.3. The spray was applied using a bi-layer dye system and an airbrush (air brush capital 2006GF). The airbrush used a gravity feed system to feed the dye using a 60 psi flow of compressed nitrogen. Spraying was performed with the airbrush approximately 15 centimeters from the laryngeal surface.

Many of the dyes produced insufficient contrast, or produced a confluent coating of the folds rather than succinct speckles. In total, I4 different dye and speckle methods were tested. India ink tended to be washed away during airflow. Humidified air displaced or entirely removed the dye. Allowing the dye to dry over periods of 5, 15 or 30 minutes did not resolve the problem. The ERA face did not produce a sufficient contrast, although it did bind to the vocal folds during oscillations. A layer of ERA face cosmetic, in combination with sprayed india ink offered satisfactory adhesion and contrast. However, this mixture was still not perfect; the dye and cosmetic were washed out in many experiments.

2.4 Experimental Apparatus

2.4.1 Flow Supply

A frame was built to hold and stabilize the larynx during airflow, hold and stabilize the camera and light sources, and to allow PVC tubing to be attached to the trachea. The frame was built using parts from Bosch Rexroth consisting of aluminum bars, plastic sliders, and steel bolts. The

camera was placed 28 cm above the vocal folds. The camera and vocal folds were fixed onto the frame using adjustable screws through the laryngeal holder, as shown in fig. 2.4. The trachea was attached to 3.2 cm PVC tubing using a hose clamp.

2.4.2 Camera

The camera used was a Canon EOS 30D Digital camera, with a sensitivity of ISO 3200, a shutter speed of 1/8000ths, and a frame rate of five frames per second (fig. 2.5). The camera was connected to a laptop to produce on-line images on the computer. The camera was equipped with a Canon Zoom Lens EF-S 17-85 mm, which allowed for increased image resolution. The resolution within the area of interest was approximately 2500 pixels. Although this was deemed acceptable for DIC analysis, a greater resolution would have been desirable in some cases.

A high sensitivity is needed to obtain the maximum possible contrast between tissue and dye. Because DIC is based on contrasts in the area of interest, a higher sensitivity leads to more accurate analysis. This is also very important due to the high shutter speed, which decreases light, reducing picture contrast.

The shutter speed of 1/8000th s (a .125 ms exposure time) was the highest speed of the camera. A short exposure time is needed in order to avoid blurriness of the vocal fold images during vibration. The vocal folds oscillate at a frequency greater than 100 Hz, yielding periods of less than 10 ms. The exposure time must be much smaller than the period. Too low shutter speed causes excessive exposure time, and blurred images.

When making a movie, the highest possible frame rate was a FPS rate of five for this camera. Given the high frequency of vibration, it was impossible to get more than a single picture from any single cycle. However, series of pictures taken with a low frame rate allowed for a stroboscopic viewof the laryngeal configuration at the different times over the cycle.

2.4.3 Light Source

The light source used was a Stocker-Yale Model 21AC with 2 semi-rigid fiber optic probes. These were placed approximately 8-10 cm away from the vocal folds to produce optimal lighting. The light beam was oriented at an angle of approximately 30 degrees with respect to the horizontal to minimize glare.

2.4.4 Air Supply

An Ametek Windjammer 14.5 cm diameter centrifugal blower was used as the flow source. A schematic of the apparatus is shown in fig. 2.5a. The blower had a maximum flow rate of 3710 liters/minute, and provided a maximum pressure rise of approximately 17 kPa. These properties are similar to anatomical conditions during phonation. The typical threshold pressure for vibration is between 300 Pa and 1 kPa. The pump was placed in a chamber lined with sound absorbing material to reduce background noise from the blower. A long anechoic termination, along with a heating and humidification system was also used. The system consisted of a large plastic container with a high water level and a submerged electronic heater. The chamber heated and humidified the air to physiological levels, with a temperature of 35-38^0 C, and a humidity

level of 98 to 100%. The water tank was sometimes bypassed in order to reduce condensation on the cords, and prevent ink dilution. Air flowed through PVC tubing into the trachea, and then the vocal folds. The humidity and temperature were recorded using a digital thermometer/hygrometer before each trial. Once the larynx was secured in the holding clamp and attached to the PVC tubing, the air supply would be turned on and raised until self-oscillation occurred.

2.4.5 Digital Images

Problems were encountered during preliminary tests. A diminished clarity of the images was noted when the vocal folds vibrated at high frequencies. Repeated adjustments were needed in order to focus the camera. The shutter speed was adjusted to its maximum value, in order to limit blurring of the image. However, it was impossible, given the limited depth of field of the camera to reduce blur along the medial edge of the vocal fold. The edge rose during oscillation, bringing this portion of the fold out of focus. This problem, associated with significant motion along the inferior-superior plane, was also reported by Spencer[31] and others.

Glare was also a major problem. Glare decreased the ability of VIC 2D to analyze the vocal fold tissue in the deformed state. Glare from the light source was greatest immediately lateral to the medial edge of the vocal fold, as shown in Fig. 2.7. Different strategies were used to reduce glare. The light beam was placed at an angle of 30 degrees with respect to the horizontal. Increasing the angle further exacerbated glare over a greater portion of the vocal fold. Decreasing the angle would not allow ample illumination of the larynx. The intensity of the light source was reduced to approximately 60% of its maximum value. Finally, a darker shade of the ERA face cosmetic was chosen, as lighter shades led to increased glare. In total, 12 larynges

were tested using the ERA face cosmetic and india ink. Two successful trials were analyzed using VIC 2D.

2.4.6 Frequency and Sound Measurements

A microphone was used to measure the radiated sound pressure. The microphone was a Brüel & Kjær 4939 (0.635 cm diameter), with a Brüel & Kjær Nexus Type 2690 conditioning amplifier to power and amplify the microphone signals. A labview 8.0 and NI USB-9233 analog input module was used for data acquisition.

2.4.7 Experimentation

Pressure and flow measurements on 6 larynges were attempted in order to verify the experimental set-up. Successful results were obtained on 4 larynges. Frequency measurements were then measured on 2 pig larynges. A total of 12 larynges were tested using VIC 2D. However, two larynges provided analyzable data. The other 10 larynges had to be eliminated from the analysis secondary to severe glare from the camera's flash, or due to the dye being washed away during airflow through the larynx.

a)

b)

c)

Figure 2.1 Excised porcine larynx (A, B) after soft tissue removal. Post-preparation (C) of the porcine larynx prior to spray and experimentation.

a)

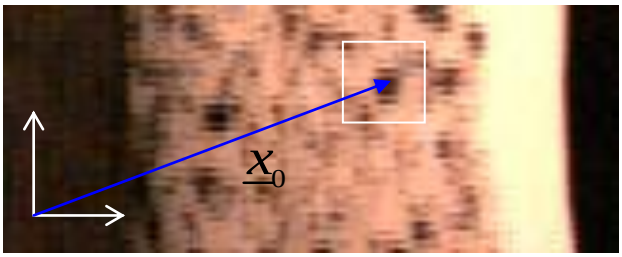

b)

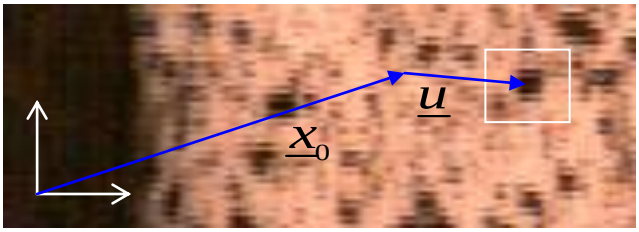

Figure 2.2. Pictures illustrating the concept of digital image correlation. $\underline{X}_0$ is the initial position of the 10 x 10 pixel subset. $\underline{U}_0$ is the displacement vector obtained by tracking the subset motion. (Images taken from M. Spencer thesis, 2008[31]).

Dye	Solvent	Spray	Gray Scale Distribution Analysis
Methylene Blue	Water	Air Brush	Poor
Methylene Blue	Water+Barium	Air Brush	Poor
Toluidine Blue	Water	Air Brush	Poor
Congo Red	Water	Air Brush	Poor
India Ink	Water	Air Brush	Successful
India Ink	Water+Barium	Air Brush	Poor
Indigo Carmine Blue	Water	Air Brush	Poor
Food dye	None	Air Brush	Poor
ERA FACE	None	Aerosol	Successful
Giemmsa Stain	Water	Air Brush	Poor
Cranberry Powder	None	Wire Mesh Screen	Poor
Blush	None	Wire Mesh Screen	Poor
Powder Foundation	None	Wire Mesh Screen	Poor
Air Brush Foundation	None	Air Brush	Poor

Table 2.1. Dyes tested, with their respective solvents, spray techniques and analysis of their grey scale distributions.

a) b)

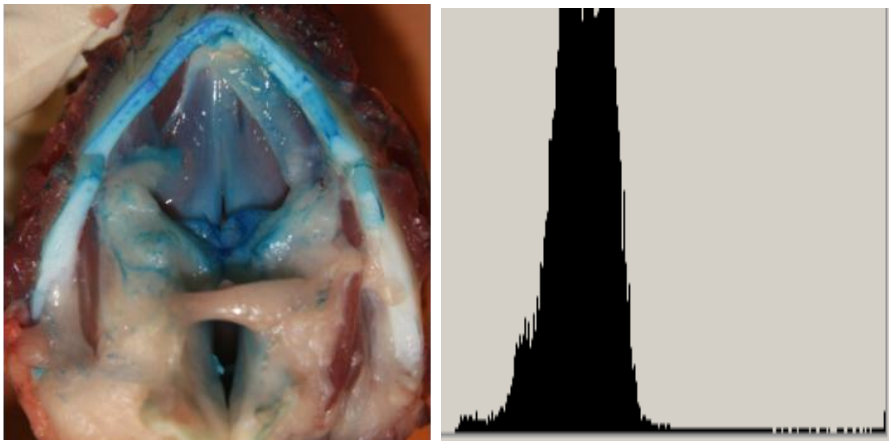

c) d)

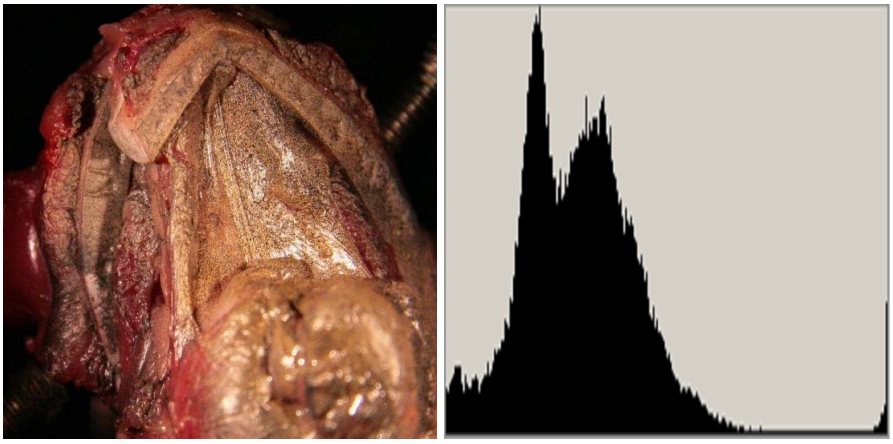

Figure 2.3 Images and grey scale distribution distribution of porcine larynges status-post spraying using methylene blue (2.3a and b) and india ink (fig. 2.3c and d). Note the diffuse infiltration of the tissues by the methylene blue and the speckling produced by india ink. Associated with the images is their respective grey scale distribution.

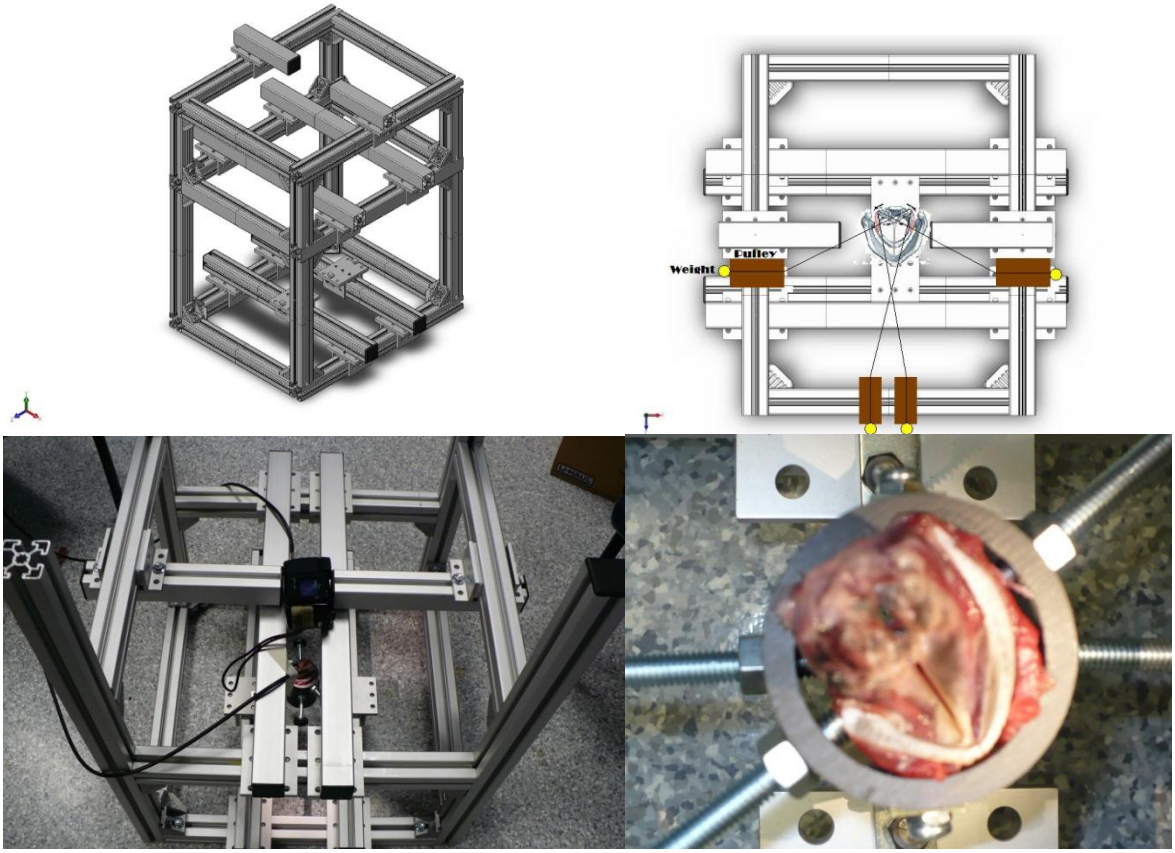

Figure 2.4 Pictures of the framework designed to hold the larynx and the camera during the measurements.

a)

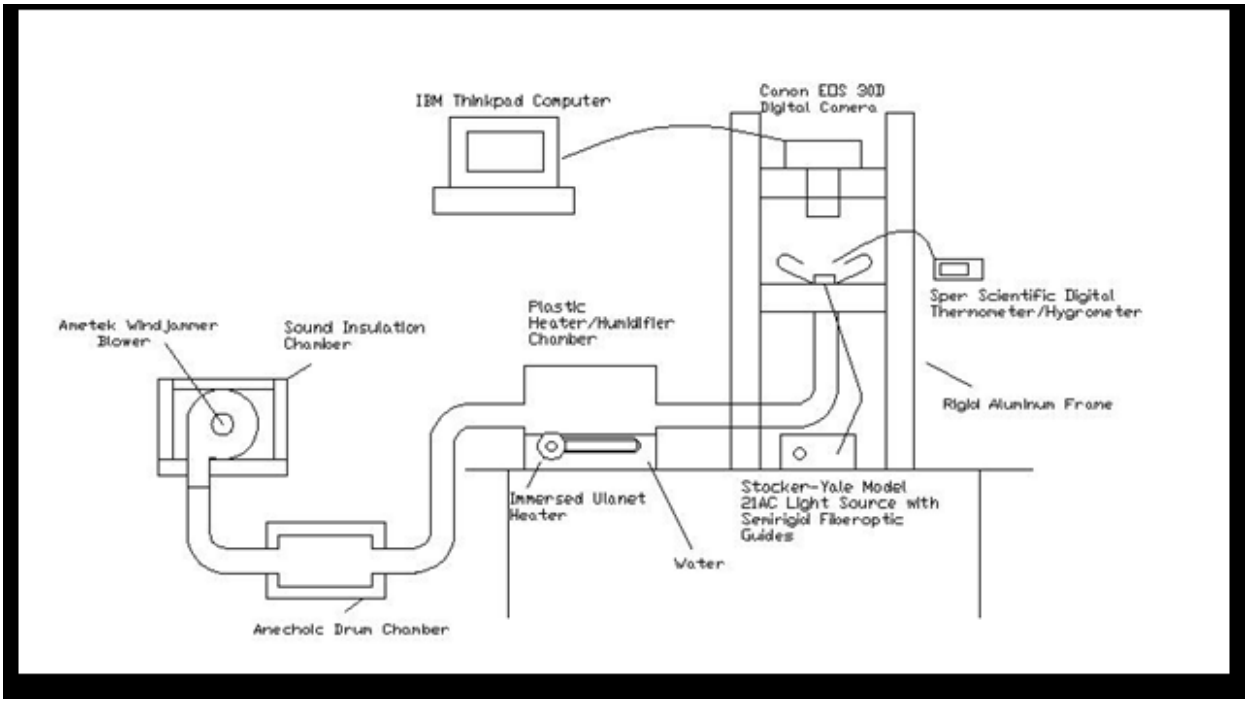

b)

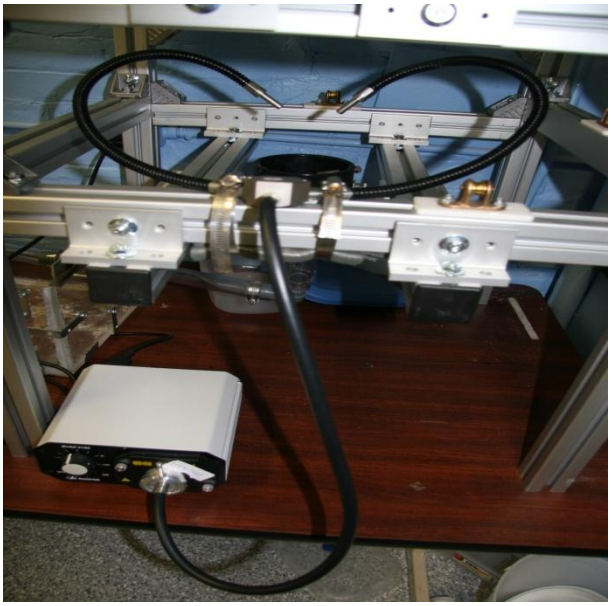

c)

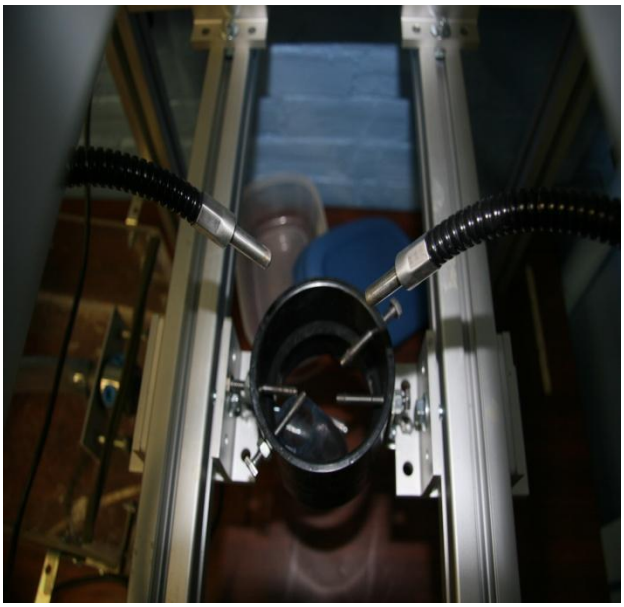

Fig. 2.5 Schematic view of the experimental apparatus (a). Pictures of the apparatus holding the larynx with associated light source (b,c).

a) b)

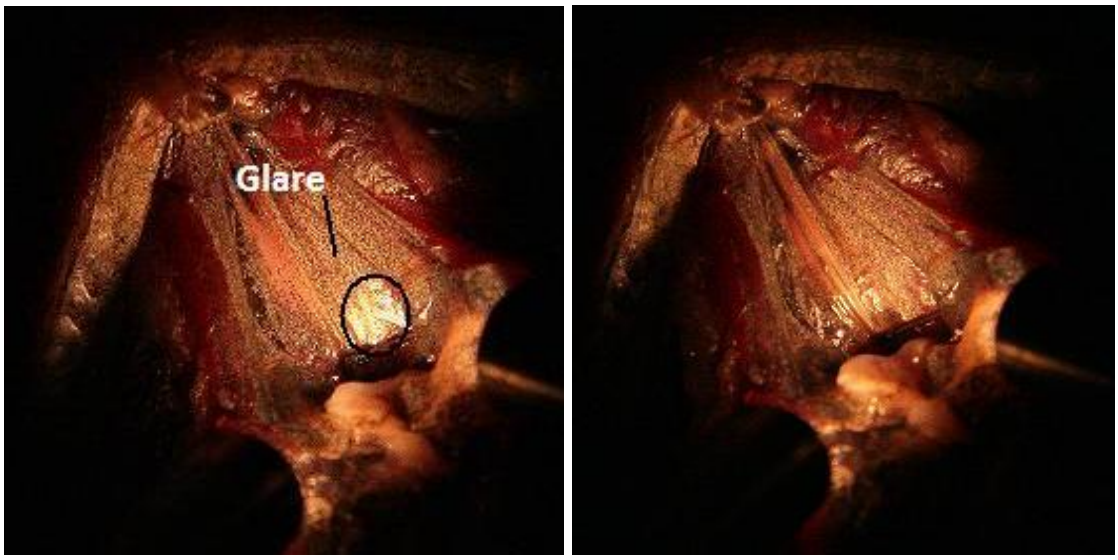

Figure 2.6 Glare produced by reflection of light source (a), with a change in light source angle pictured on the right (b).

CHAPTER 3: Results

3.1 Experimental Results

3.1.1 Mean Pressure and Flow Measurements

In order to verify the experimental set-up, pressure and flow rate measurements were made and compared to results for a similar experimental protocol and design performed by Alipour on bovine larynges (Fig. 3.1). The flow was increased in small increments. The threshold pressure was measured along with the time-average flow rate. Measurements were performed while increasing and decreasing flow rate to capture hysteresis. Results are shown in fig. 3.1. Below onset, the pressure continuously built up in the subglottic region. When the flow was high enough to reach onset, oscillations occurred as air flowed intermittently through the glottis. Oscillation onset resulted in a drop in subglottic pressure as shown in fig. 3.2. For larynx 4 (fig. 3.1), the vocal folds began to oscillate once the flow reached approximately 510 ml/s. Consistent results were obtained for four of six separate larynges (fig. 3.2). Two larynges were eliminated due to the specimens inability to oscillate. The pressure recorded while the flow rate was diminished was observed to be consistently lower than the pressure observed while the flow rates was increased. Such a trend was observed for all larynges tested, and is also consistent with Alipour's model[29]. For example, the pressure recorded while the flow rate was increased was greater than when the flow rate was reduced for around 400 ml/s,. As the flow rate was increased and reached 400 ml/s (the upper portion of the blue curve), the pressure recorded was approximately 10 Kpa. As the flow was reduced (the lower portion of the blue curve), the pressure was only 8 cm H_2O. The system exhibits flow rate independent memory, termed hysteresis. This phenomenon will be described in the discussion section.

3.2 Frequency of Vibration Measurements

Fig. 3.3 represents a typical frequency spectrum of the sound radiated by the vocal folds. The fundamental frequency was 272 Hz. The fundamental frequencies observed for the five porcine larynges tested were between 250 to 300 Hz. The first three harmonics of the fundamental frequency were also significant. Harmonics of the fundamental frequency are multiples of the fundamental frequency for a periodic waveform.

3.3 DIC Measurements

Deformation data was obtained for two larynges. The reference image utilized was the vocal fold at rest, prior to air flow, with the larynx sutured. Images for the two cases are shown in fig. 3.4. As can be seen in these photographs, there is successful dye adherence to the laryngeal surface as air is flowing through the larynx. Minimal glare was obtained.

3.3.1 First Animal Model

A colored diagram representing the x and y components of strain occurring in the deformed state is shown below in fig. 3.5, as created by the VIC 2D computer software. Strain values were analyzed and calculated over the area shown. The color spectrum ranges between orange and purple. Orange represents a stretching of the tissue of 2.8%. The blue and darker regions identified by the arrows represent areas of compression, as indicated by the negative principal strain values. The largest area of compressive strain values approach -6.1%. This occurred at the

most medial region analyzed, near the free edge of the vocal fold. Other portions of the vocal fold could not be analyzed because of glare or dye washout.

Stress values may be estimated from the strain values obtained from the VIC 2D software if the Young's modulus is known. Young's modulus was assumed to be 22 kPa, previously described by Alipour[19]. The shear modulus (G) can be calculated from Young's modulus,. Stress was then calculated using the following equations:

1. $$G = \frac{E}{2 + 2\nu}$$

2. $$\sigma_{xx} = G\ (4\varepsilon_{xx} + 2\varepsilon_{yy})$$

where G is Shear modulus, E is Young's modulus, ν is Poisson ratio, σ_{xx} is stress, ε_{xx} is strain in the X plane, and ε_{yy} is strain in the Y plane.

Maximum and minimum stress values along the X (antero-posterior) and Y (medial-lateral) plains were calculated using the above formula's. Stress values are reported in table 3.1.

3.3.2 Second Animal Model

For the second animal model, the vocal fold excursion was lateral in its excursion compared to the previous case. Fig. 3.6 shows the region of analysis, and the associated X (antero-posterior)

and Y (medial-lateral) component strains. The strain was negative in the entire region of analysis. The values ranged from -18% to -4.5%. This indicates that the forces acting on the tissue were compressive. As for the first model, calculations of stress were performed. The results are shown in table 3.2. Please note the large negative strain values obtained in the medial-lateral direction.

3.4 Average Strain

Time averaged strains were calculated and plotted in fig. 3.7 to quantify the compressive strain of the tissues over one complete oscillatory cycle. Maximal negative strain values were observed when the vocal folds were in their most lateral position during oscillation, representing the maximal amplitude (distance from the midline).

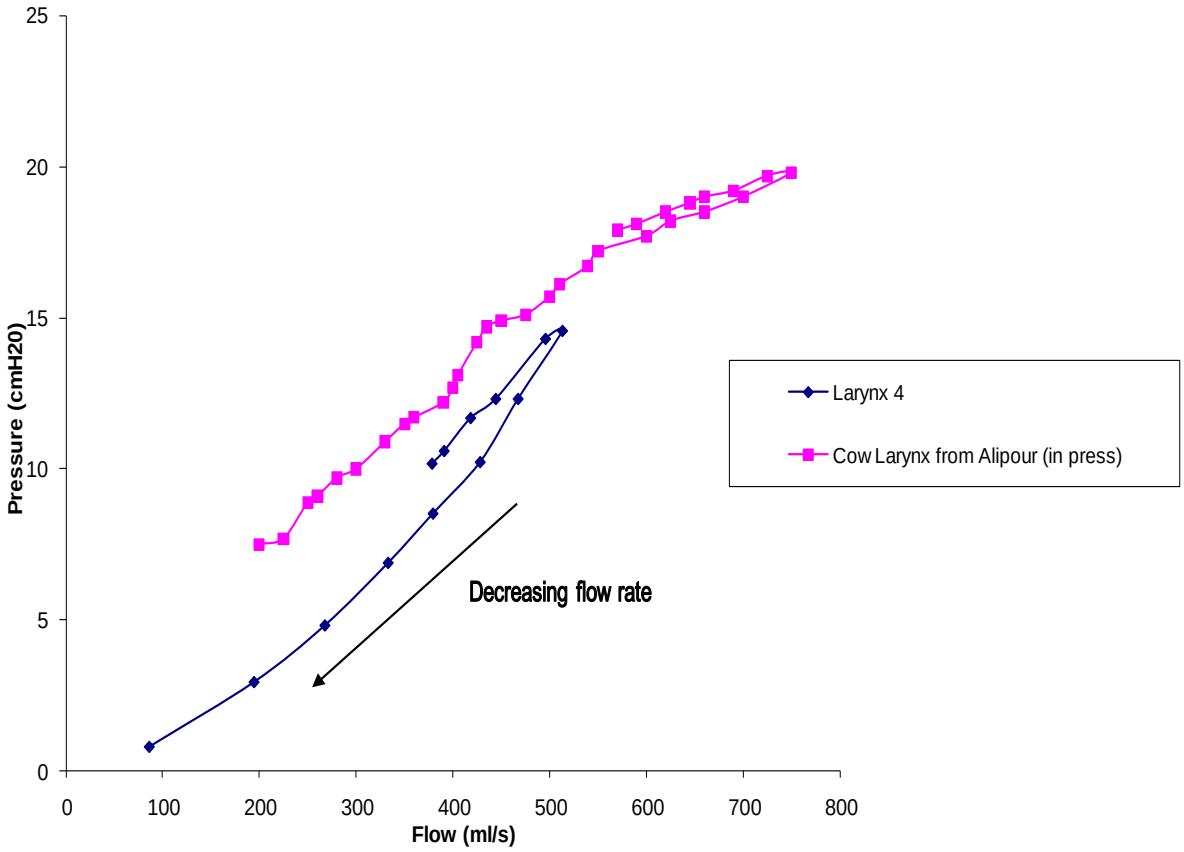

Figure 3.1 Pressure versus flow rate measurements in a porcine (blue) and bovine (pink) cadaveric larynx. The blue line represents Larynx 4, while the pink line represents data from a cow larynx from Allipour (in press).

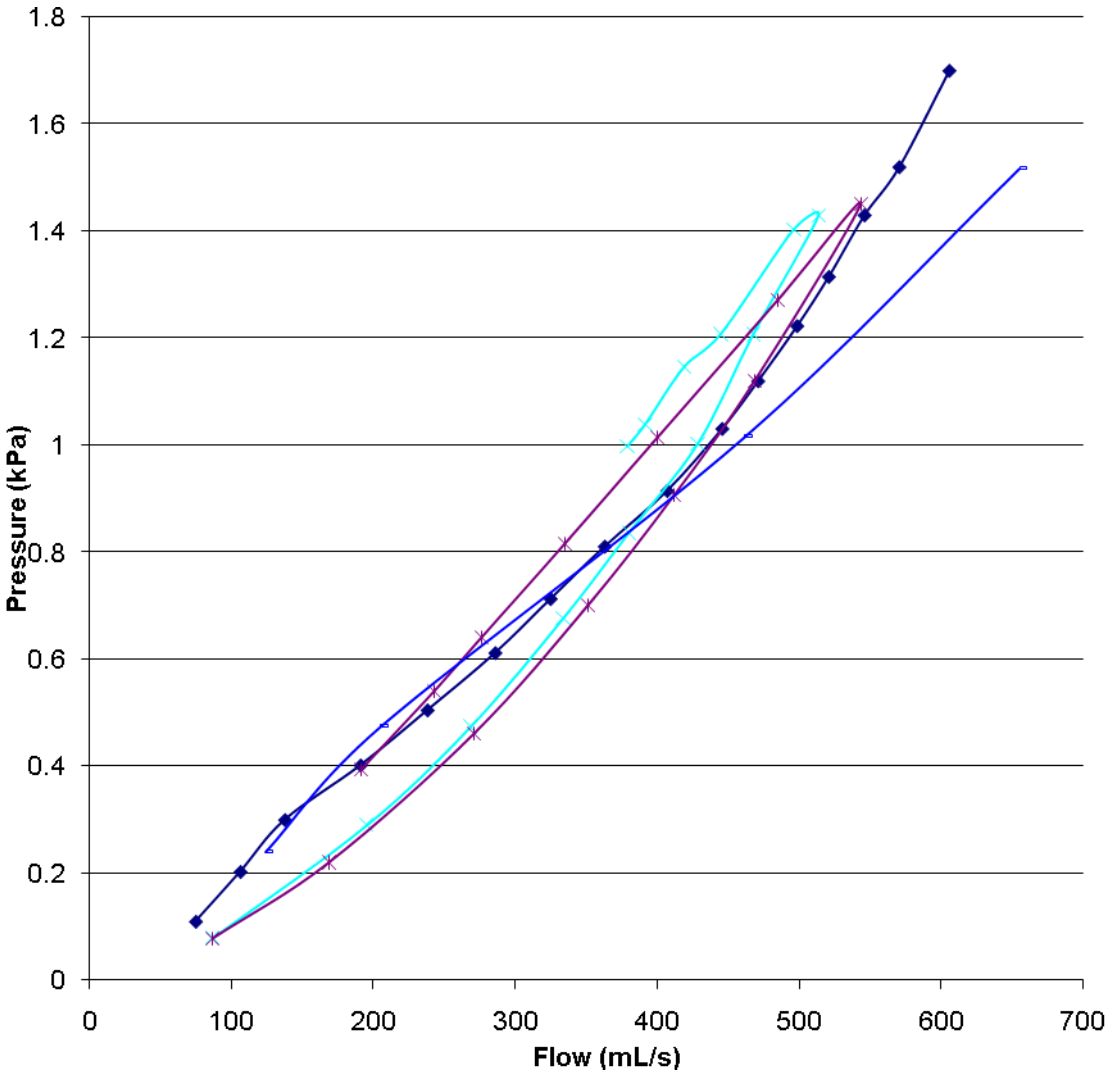

Figure 3.2 Pressure versus flow rate which is displaying similar elevations in pressure with increasing of the flow during four separate trials. Results from 3 Larynges (Larynx 1, 4, and 6) were attained. Note that 2 trials are attained using the larynx 4. Legend:

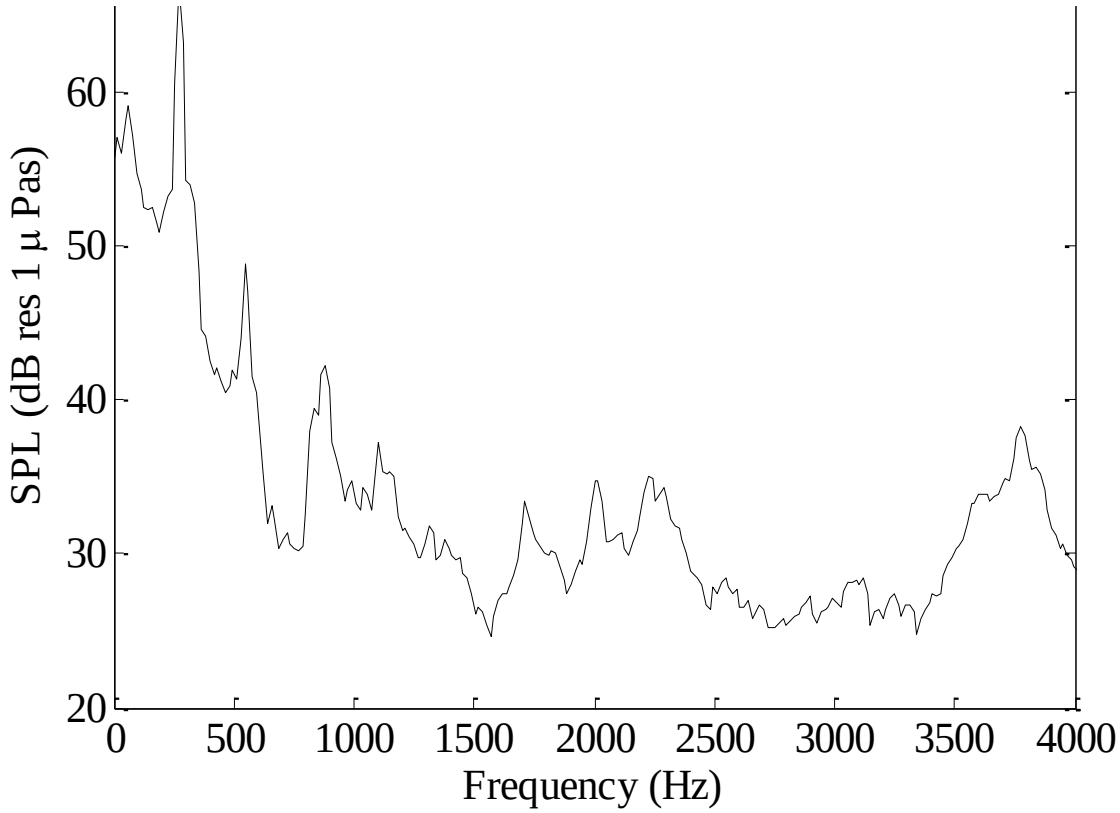

Figure 3.3 Frequency spectrum of the radiated sound in the first animal model. Peaks representing the fundamental frequency and harmonics are observed at 272 Hz, 546 Hz, 820 Hz and at 1150 Hz.

	Trial 1	Trial 2
At rest (reference)		
Oscillating		

Figure 3.4 Images obtained of vocal folds at rest and oscillating during 2 successful trials of Digital Image Correlation.

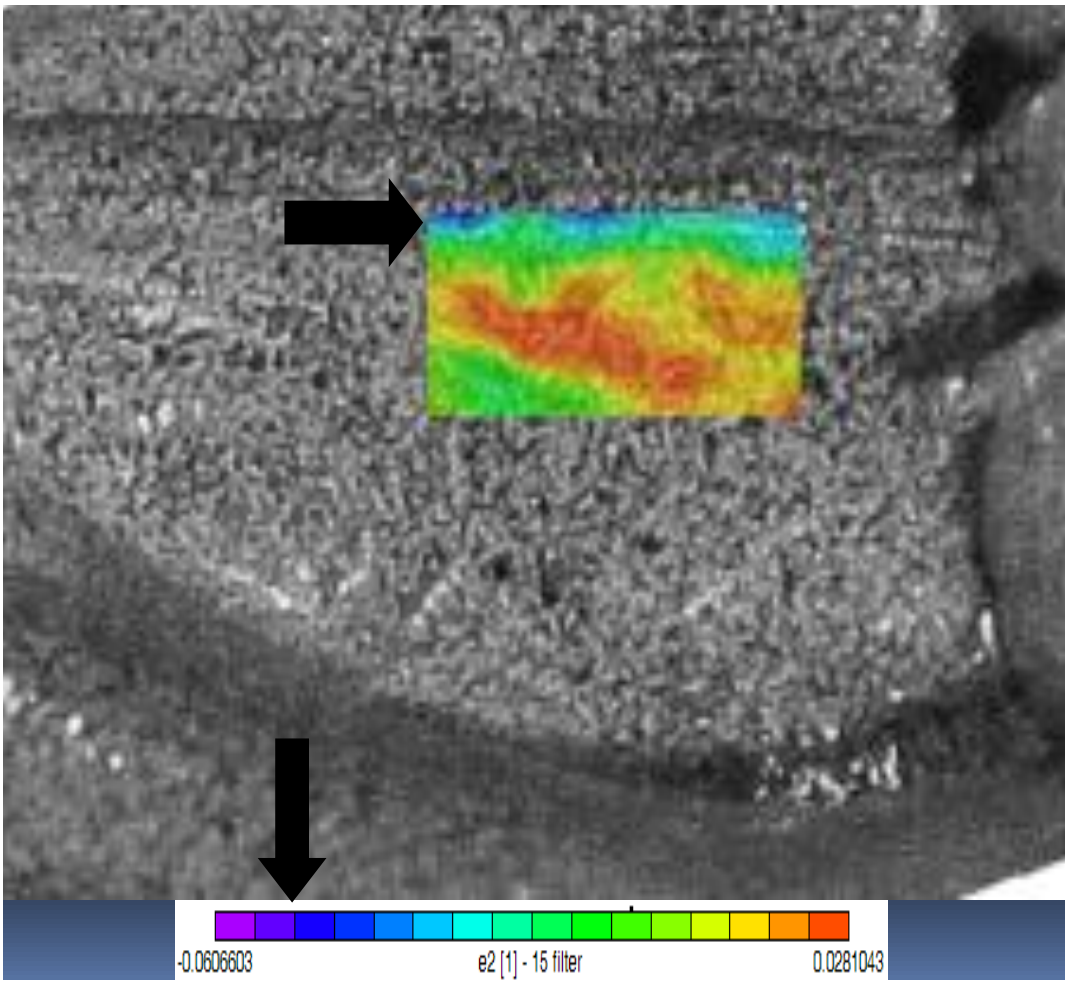

Figure 3.5 Color diagram of principal strain measurements of trial #1. Note the strains reach levels of -6.1% to 2.8%.

Stress (kPa)	Trial 1
A-P max	2.45
A-P min	-1.10
M-L max	2.97
M-L min	-1.53

Table 3.1 Maximum and minimum stress values of trial #1, using the equation: Stress (σ_{xx}) = G ($4\varepsilon_{xx} + 2\varepsilon_{yy}$).

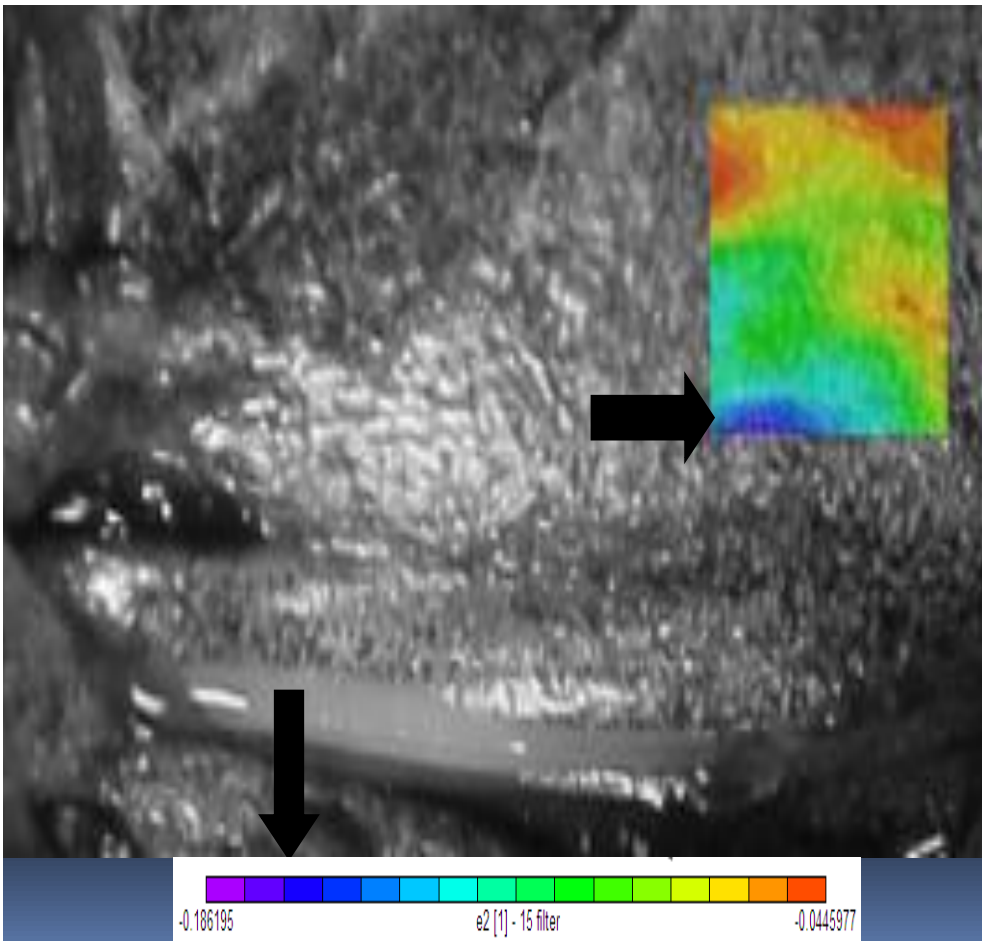

Figure 3.6 Color diagram of principal strain measurements of trial #2. The values range from -18% to -4.5%, thus demonstrating that only compressive forces are acting on the tissues being analyzed.

n

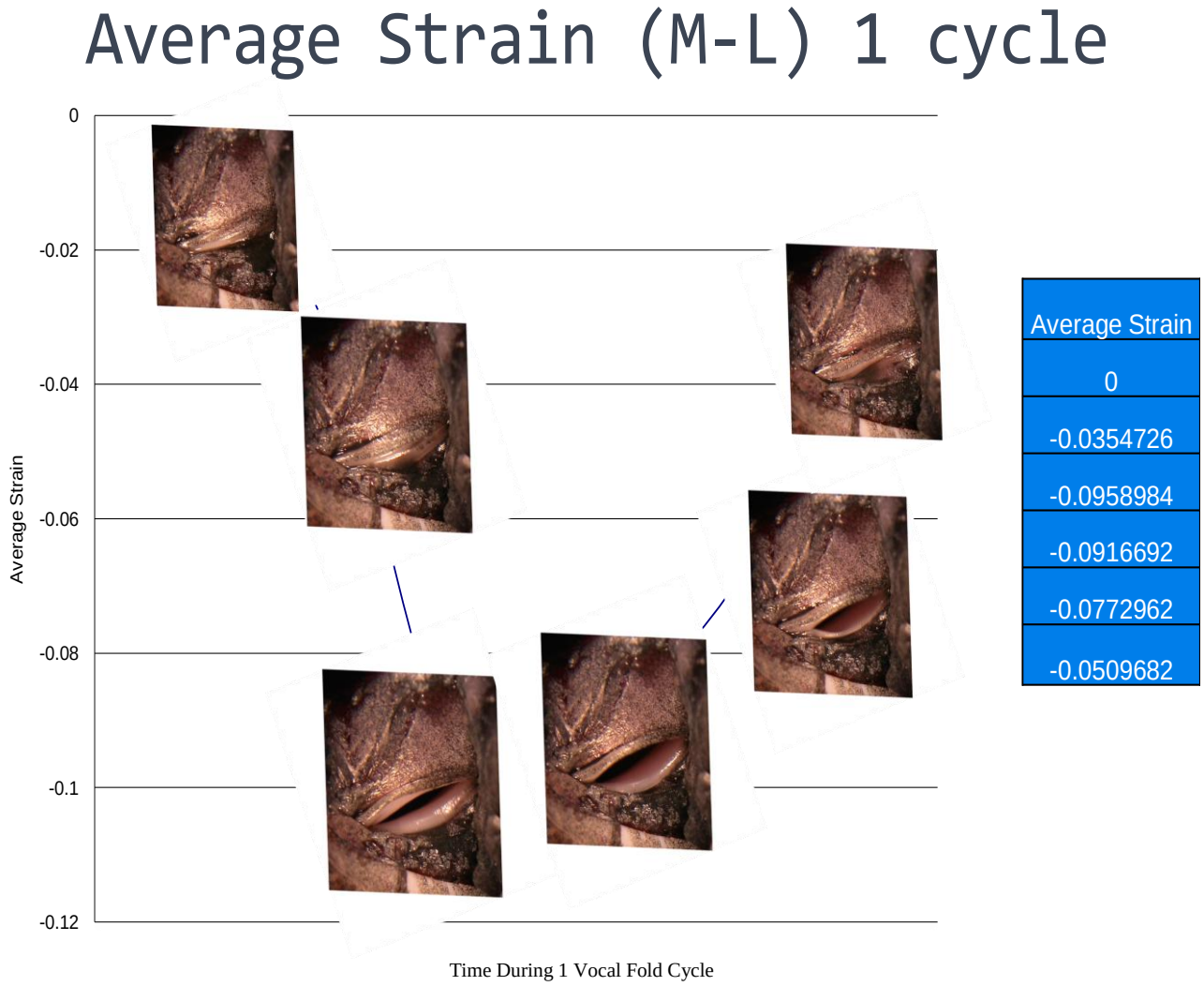

Figure 3.7 Average strain in the porcine vocal fold of trial #2 one entire oscillatory cycle. Numbers in blue table on the right correspond sequentially to the pictures located in the figure.

Stress (kPa)	Trial 2
A-P max	0.06
A-P min	-3.26
M-L max	-0.95
M-L min	-5.64

Table 3.2 Maximum and minimum stress values, using the equation:
Stress (σ_{xx}) = G ($4\varepsilon_{xx} + 2\varepsilon_{yy}$).

CHAPTER 4: Discussion

4.1 Fundamental Frequency

Human vocal folds oscillate at approximately 220 Hz in women, and 120 Hz in men. The elevated fundamental frequency in our cases which measured between 250 and 300Hz may have multiple explanations. Alipour concluded that the fundamental frequency of the pig was between 100 and 300 Hz, the higher levels likely representing the natural squeal of the pig's voice. Thus, the higher frequencies observed during our experiments might be a true representation of the pigs voice. Additional factors may have also influenced the elevated fundamental frequency. The frequency range noted during Alipour's experiments depended on tension forces applied to the lateral cricoarytenoid muscle. As the tension increased, the fundamental frequency increased. Our model included suturing the vocal folds together near the posterior aspect of the free vibrating edge, or directly anterior to the vocal process. This naturally placed the vocal folds in a tensed state. External forces were applied to the laryngeal skeleton which held the larynx in position may have slightly further raised the tension of the vocal folds.

4.2 Pressure-Flow Measurements

Hysteresis was observed during pressure versus flow rate experimentation on all the samples tested. Subglottic pressure was recorded while the flow was increased past the onset pressure for oscillation, and while the flow was decreased. The pressure recorded was greater during the rise in flow prior to oscillation as compared to the pressure recorded while the flow was diminished after vocal fold oscillations. The vocal folds therefore include a time dependant factor during

phonation. Hysteresis is commonly observed in post-mortem laryngeal experiments due to viscoplastic and viscoelastic properties of the tissues[19, 20].

An increased elasticity in the composition of tissues would decrease the hysteretic effects, whereas a decrease would cause increased stiffness and plasticity, which would lead to increased time dependence. A material that displays viscoplasticity will not fully recover the original length or shape of the material. A viscoelastic material would recover the shape, however not immediately. Therefore, as the stresses and strains on the vocal folds increase due to increased pressure, the material deforms and the vocal gap is increased. When the pressure is decreased, the gap is larger and the resistance to flow is decreased. Therefore higher flow rates are achieved at lower pressures.

An additional variable that adds to the hysteresis is the use of post mortem excised larynges. The tissue is not able to maintain its mechanical properties outside of the measures taken in the experiment. Although the larynges are initially moist, the vocal folds will dry out over time. The dryness will also greatly increase as air is passing through the larynx. When the vocal folds dry, they become increasingly stiff and lose their elastic properties. Increased plasticity will result, which will again decrease the resistance to air flow as the pressure is decreased.

4.3 Stress-Strain Results

The goal of the current study was to create a method of measuring vocal fold superior surface strains using digital imagery correlation, and to calculate the stresses from the strain using

Young's modulus. The appealing advantage of this technology is that it would be tolerable for the patient. To date, most in-vivo studies utilize technologies that require trans-oral and oral-pharyngeal placement of instruments, which leads to improper placement of pressure transducers between patient's vocal folds, and/or gag/cough reflexes. Such a method of measurement has only seen success in approximately half its subjects[23, 24] (fig. 4.1). Digital Imagery correlation would be an easier procedure to undergo, with local freezing agents providing enough anesthetic to allow adequate patient comfort. In addition, the entire surface of the fold could be measured. Transoral instrumentation only measures the location where the probe is placed.

The results from the DIC analysis show a pattern intuitive to the motion of the vocal folds. The pixel areas of the two trials are slightly different, so the absolute pixel displacement is not as important as the pattern and distribution seen when comparing the two trials. However, the principle strain is dimensionless, and can thus be compared between the two trials. The largest pixel displacement is towards the medial third portion of the folds, where the displacement is largest. The first animal trial analysis occurs at an early point during oscillation, when the onset pressure has just been met, and the glottis gap is minimal. The second trial shows the distribution when the folds are at their maximum excursion. A maximum principal strain value of -0.186 is seen in trial 2, as compared to a value of -0.0606 in the first trial. When analyzing the area of interest in both trials, the observation is made that the most elevated strain values occur toward the most medial portion of the true vocal fold. In addition, the largest amounts of displacement (strain) occur closer to the medial third of the true vocal fold.

Due to the proportionality of the relationship of stress and strain, most of the stress values calculated are compressive (a negative value is obtained after calculations are performed using strain values in the X and Y planes). In trial 1, the stress values in the medial-lateral direction are

in the order of 2.97 to – 1.53 kPa, and the anterior-posterior direction is 2.45 to -1.10. In animal trial 2, the maximal and minimal medial-lateral stress values obtained are -0.95 to -5.64 kPa, whereas the maximal and minimal stress values in the anterior-posterior direction are 0.06 to -3.26 kPa. Intuitively, the values of stress in the medial-lateral direction are much greater in the second trial, as it is closest to the amplitude of the folds lateral excursion. Anterior-posterior values are similar in absolute size in the two trials. However, they are mostly compressive in the second trial, whereas they are tensile and compressed in trial number 1.

How do these values compare with the previous literature on this subject? In a study using a physical model of the vocal folds[17], stress found during the closed phase of oscillation was tensile, which is attributed to the model vocal folds stretching in the medial-lateral direction in order to overcome the glottal gap. The results also show a reduced (less tensile) stress state near the area of contact on the model vocal folds. Results from this study are in agreement with the data showing the lowest (most compressive) strain toward the medial edge of the vocal fold.

Differences in strain fields may be due to the vibration of the physical model varying from that of excised larynges. The physical model strain field was obtained using 3-D DIC while the strain field in this study used 2-D DIC. Small differences in results from 2D and 3D DIC have been observed[17].

In cadaveric animal studies[13, 14], peak pressures were recorded in the range of 3 kPa. These absolute values are once again similar to the absolute values obtained on the superior surface of the true vocal folds in the present study under discussion. In addition, in the study by Jiang and titze, where 3 different locations were recorded along the horizontal length of the vocal folds, it was noted that peak pressures occurred along the middle third of the fold. This is consistent with

the results of the present study, where the analysis displayed similar elevated stresses and strains on the true vocal folds.

In human studies previously performed[21, 22], peak pressures in the order of 1-3 kPa were noted across 3 human subject trials. Again, this is consistent with the data in the present study. In addition, increases in intensity noted with elevated decibel levels recorded displayed a proportional relationship with contact pressure. Such a comparison was not performed in the present study.

Thus, the absolute values attained of contact pressures by previous research groups using various models, including rubber models, cadaveric larynges, and in-vivo subjects are similar in value to the ones attained in the present study. Further work into the stresses and strains on the medial edge of the vocal folds (using VIC 3D), with comparisons using pressure transducers, will elucidate whether impact pressures can be elucidated from the superior surface stresses and strains measured with digital imagery correlation.

4.4 Clinical correlation

To the clinical otolaryngologist, the most important question that needs answering is if this data correlates to the clinical picture observed in nodules, polyps and cysts. These lesions usually occur at the areas of maximal impact, which is felt to be along the middle third of the true vocal fold. In reviewing the results of principal strain obtained in the 2 trials, the observation that is expected is obtained. As the true vocal fold makes its lateral excursion during phonation, the tissue is compressed, causing the speckles to cluster together, and the measurement made by VIC 2D displays negative strain. This is the trend viewed in both trials.

More interestingly, the location where this compression is largest occurs nearest to the middle third of the true vocal fold (see white arrows, fig. 4.2). Although successful analysis was not performed directly at the medial surface, the trend of our two successful trials appears to show peak values near the middle third. These results are further validated when observing the stress values in table 2 and table 3. The values in the medial-lateral direction (Y-plane) are primarily negative, and larger in the second trial, where the comparison is made when the vocal fold is at the most lateral portion of its oscillation.

In addition, the average strain graft of fig. 3.7 displays increasing strain as the vocal fold undergoes its excursion from medial to lateral. The average strain values become increasing more negative, indicating further compression of the tissues. This is important to the clinician, because the further lateral the excursion of the vocal fold is during phonation, the greater are the strains on the tissue. If the excursion could be limited by a speech pathologist, perhaps by decreasing subglottic pressures during phonation, this may lead to diminished strain. Further trials, including human in-vivo trials, may be able to answer this question.

The use of Digital Image Correlation for detecting inclusions in the vocal folds was investigated in a physical vocal fold model[17]. A physical model with a superficially located mass on the medial surface was constructed and its mechanical stress state during self-oscillation was compared against a baseline model. In the lesion model it was found that the superior surface medial-lateral strain and stress were reduced during collision. This was attributed to the nodule acting like a support for the vocal folds in the closed phase. The contact pressure for the lesion model was relatively constant with respect to flow rate, while the contact pressure for the baseline model was lower at low flow rate. A second lesion model with an embedded inclusion (as opposed to a superficial lesion) was also compared against a baseline. The embedded

inclusion could not be detected from the stress and strain fields obtained from Digital Image Correlation.

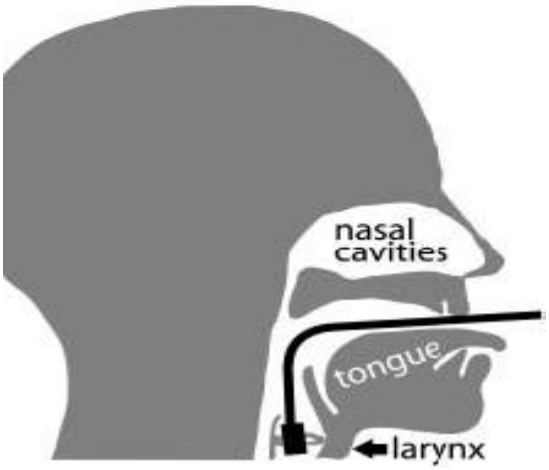

Figure 4.1 Trans-oral pressure transducer placed directly on subject's true vocal folds (Used with permission from Gunter et al., 2005).

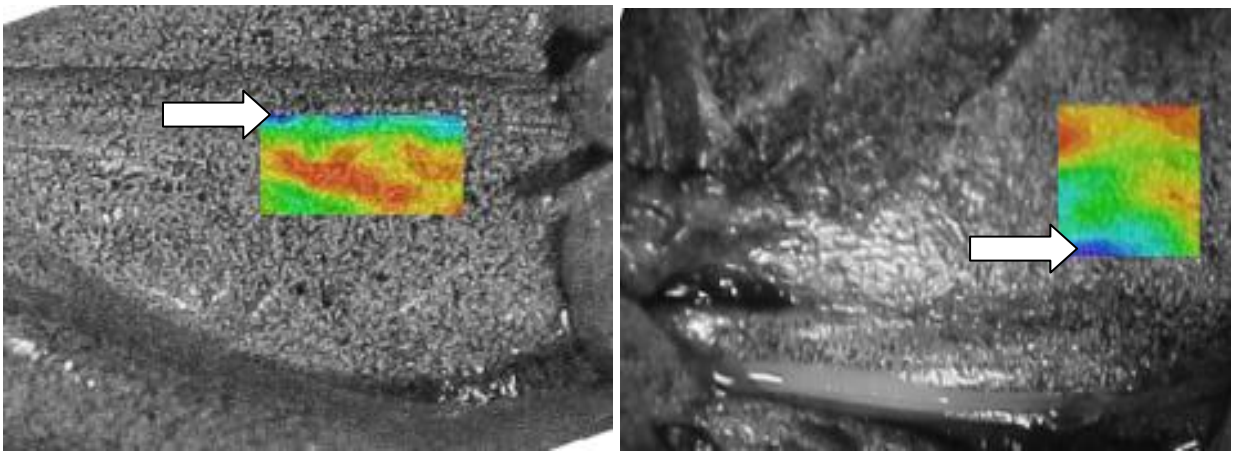

Figure 4.2 Color diagram of principal strain measurements of trial 1 and 2. Arrows point to the areas of maximal compression/strain.

CHAPTER 5: Conclusion and Future Studies

5.1 Conclusions

Digital Image correlation was used for the measurement of vocal fold impact stress in animal models. Results were consistent with data from pressure sensors placed directly between the vocal folds or vocal folds made to vibrate against plexiglass structures which held pressure sensors in place. Issues with the current experimental set-up include glare, photography limitations, dye wash-out, tissue drying, experimental apparatus design flaws and medial surface measurements. These issues will have to be experimented on in order to provide more consistent results. However, This thesis has brought an aanimal model to the stage where quantitative engineering measurements of vocal fold trauma can be made. As a result, a major step forward has been taken towards the development of a clinical method of assessing vocal trauma.

5.2 Future Studies

A new technology that will aid in the analysis of vocal fold oscillations and medial surface impact pressures is the advancement of the computer software to include measurements in 3 planes. The creation of VIC 3D using high speed cameras will allow analysis of medial edge motions.

Cadaveric human larynges are the next step in the use of this technology. Prior to in-vivo studies, further testing with either India ink alone or other non-toxic dyes must be performed. ERA face cosmetics contain toxic chemicals to the lungs, and thus its use in this application is limited to laboratory research experiments. Finally, high speed images using high speed cameras

that take photographs in excess of 5000 photographs per second will provide better resolution of the images, and gain further knowledge into studying the mucosal wave.

Clinical application of such a technology would be invaluable to the otolaryngologist. Impact pressure measurements could be instrumental in changing voice abuse through speech therapy. Such knowledge could help professionals who use their voice in their daily lives, including professional singers, whose careers are often hampered by the appearance of nodules, polyps or cysts on the medial surface of their true vocal folds. Such a technology could be useful to monitor a patient's progress once a nodule, polyp or cyst has appeared. In addition, it could be used to avoid excessive pressures in the concerned professional voice user who would like to take care of their voice prior to any pathology occurring, much like a person who is healthy runs or eats healthy to avoid future heart conditions.

CHAPTER 6: References

1. Johns MM. Update on the etiology, diagnosis, and treatment of vocal fold nodules, polyps, and cysts. *Current Opinion in Otolaryngology & Head & Neck Surgery* 11(6):456-61, 2003.
2. Aronsson C, Bohman M, Ternstrom S, Sodersten M. Loud voice during environmental noise exposure in patients with vocal nodules. *Logopedics, Phoniatrics, Vocology*. 32(2):60-70, 2007.
3. Pontes P, Kyrillos L, Behlau M, De Biase N, Pontes A. Vocal nodules and laryngeal morphology. *J Voice*. 16(3):408-14, 2002.
4. Chernobelsky SI. The treatment and results of voice therapy amongst professional classical singers with vocal fold nodules. *Logopedics, Phoniatrics, Vocology*. 32(4):178-84, 2007.
5. Garrett CG, Ossoff RH. Phonomicrosurgery II: surgical techniques. *Otolaryngologic Clinics of North America*. 33(5):1063-70, 2000 Oct.
6. Courey MS, Shohet JA, Scott MA, Ossoff RH. Immunohistochemical characterization of benign laryngeal lesions. *Ann Otol Rhinol Laryngol* 105:525–531, 1991.
7. Roy N, Merrill RM, Gray SD, et al. Voice disorders in the general population: prevalence, risk factors, and occupational impact. *Laryngoscope.* 2005;115(11)
8. Behrman A, Sulica L. Voice rest after microlaryngoscopy: current opinion and practice. *Laryngoscope.* 2003;113(12):2182–2186.
9. Behlau M, Oliveira G. Vocal hygiene for the voice professional. *Curr Opin Otolaryngol Head Neck Surg.* 2009;17(3):149–154

10. Gray SD, Titze I, Lusk RP. Electron Microscopy of Hyperphonated Canine Vocal Cords. J *Voice*. 1987;1:109–115.
11. Gray SD, Titze IR. Histologic investigation of hyperphonated canine vocal cords. *Ann Otol Rhinol Laryngol.* 1998 Jul–Aug;97:381–388.
12. Rousseau B, Ge PJ, French LC, et al. Experimentally Induced Phonation Increases Matrix Metalloproteinase-1 Gene Expression in Normal Rabbit Vocal Fold. *Otolaryngol Head Neck Surg.* 2008;138:62–68.
13. Marcotullio D, Magliulo G, Pietrunti S, Suriano M. Exudative laryngeal diseases of Reinke's space: a clinicohistopathological framing. *J Otolaryngol* 31:376–380, 2002.
14. Wohl DL. Nonsurgical management of pediatric vocal fold nodules. *Archives of Otolaryngology -- Head & Neck Surgery*. 131(1):68-70; 71-2, 2005.
15. McCrory E. Voice therapy outcomes in vocal fold nodules: a retrospective audit. International J of Lang & Com Disord. 36 Suppl:19-24, 2001.
16. Behrman A, Sulica L. Voice rest after microlaryngoscopy: current opinion and practice. Laryngoscope. 113(12):2182-6, 2003.
17. Titze IR: Mechanical stress in phonation. J Voice 1994, 8:99–105.
18. Uloza V, Saferis V, Uloziene I. Perceptual and acoustic assessment of voice pathology and the efficacy of endolaryngeal phonomicrosurgery. Journal of Voice. 19(1):138-45, 2005 Mar.
19. Robb, J. Study of Impact Stress in Physical Models and Human Subject Vocal Folds from High-Speed Video

20. Popolo PS and Titze. IRQualification of a quantitative laryngeal imaging system using videostroboscopy and videokymography. The Annals of otology, rhinology, and laryngology 117(6):404-12, 2008
21. Gunter HE. A mechanical model of vocal-fold collision with high spatial and temporal resolution. J of the Acoust Soc Am. 113(2):994-1000, 2003.
22. Jiang J, Titze I. Measurement of Vocal Fold Intraglottal Pressure and Impact Stress. J of Voice. 8 (2) 132-44, 1994
23. Verdolini K. Hess MM. Titze IR. Bierhals W. Gross M. Investigation of vocal fold impact stress in human subjects. Journal of Voice. 13(2):184-202, 1999.
24. Gunter HE, Howe RD, Zeitels SM, Kobler JB, Hillman RE. Measurement of vocal fold collision forces during phonation: methods and preliminary data. Journal of Speech Language & Hearing Research. 48(3):567-76, 2005.
25. Hess MM, Verdolini K, Bierhals W, Mansmann U, Gross M. Endolaryngeal contact pressures. Voice 12(1):50-67, 1998
26. Jiang, J. J., Shah, A. G., Hess, M. M., Verdolini, K., Banzali, F. M., and Hanson, D. G. Vocal fold impact stress analysis. J Voice 15, 4-14, 2001
27. Branski, R. C., Perera, P., Verdolini, K., Rosen, C. A., Hebda, P. A., and Agarwal, S. Dynamic biomechanical strain inhibits IL-1_-induced inflammation in vocal fold fibroblasts. J Voice 21, 651-660, 2007.
28. Verdolini, K., Chan, R., Titze, I. R., Hess, M., and Bierhals, W. Correspondence of electroglottographic closed quotient to vocal fold impact stress in excised canine larynges. *J Voice* 12, 415-423. 1998.

29. Alipour F, Jaiswal S. Phonatory characteristics of excised pig, sheep, and cow larynges. *J Acoust Soc Am* 123(6): 4572-81, 2008.

30. Thomson, S. L., Mongeau, L., and Frankel, S. H. Aerodynamic transfer of energy to the vocal folds. *J Acoust Soc of Am*. 118:1689-1700, 2005.

31. Spencer, M. Siegmund T, Mongeau L. Determination of superior surface strains and stresses, and vocal fold contact pressure in a synthetic larynx model using digital image correlation. *J Acoust Soc Am*. 123 (2) 1089-1103, 2008.

32. LI JEN Investigations of mechanical stresses within human vocal folds during phonation

33. Zhang, DS, Eggleton, CD. Arola, DD. Evaluating the mechanical behavior of arterial tissue using digital image correlation. Experimental Mechanics. 42 (4). 409-416

34. Sutton MA, Ke X, Lessner SM, et al. Strain field measurements on mouse carotid arteries using microscopic three-dimensional digital image correlation. *J Biomed Material* 84A (1) 178-190, 2008.

35. Zhang, Kai, and Thomas Siegmund. A constitutive model of the human vocal fold cover for fundamental frequency regulation. The Journal of the Acoustical Society of America 119 (2006): 1050-062.

36. Tippler, P. Physics for Scientists and Engineers: Mechanics, Oscillations and Waves, Thermodynamics (5th ed. ed.), 2004